Agricultural Water Management 213 (2019) 792–802

Contents lists available at ScienceDirect

Agricultural Water Management

journal homepage: www.elsevier.com/locate/agwat

A coupled model for simulating water flow and solute transport in furrow irrigation

Kun Liu[a,b], Guanhua Huang[a,b,*], Xu Xu[a,b], Yunwu Xiong[a,b], Quanzhong Huang[a,b], Jiří Šimůnek[c]

[a] Center for Agricultural Water Research, China Agricultural University, Beijing, 100083, China
[b] Chinese-Israeli International Center for Research and Training in Agriculture, China Agricultural University, Beijing, 100083, China
[c] Department of Environmental Sciences, University of California Riverside, Riverside, CA 92 521, USA

ARTICLE INFO

Keywords:
Surface irrigation
Solute transport
Mathematical model
Coupling procedure

ABSTRACT

For optimal water and fertilizer management under furrow irrigation, it is important to understand the water and solute dynamics on the land surface and in the subsurface. An efficient mathematical tool is required to describe these dynamic processes. We propose a coupled model in which surface water flow and solute transport are described using the zero-inertia equation and the average cross-sectional convection-dispersion equation, respectively, while the two-dimensional Richards equation and the convection-dispersion equation are used to simulate water flow and solute transport in soils, respectively. Solutions are computed numerically using finite differences for surface water flow and finite volumes for solute transports in furrow. Subsurface water flow and solute transport equations are solved using the CHAIN_2D code. An iterative method is used to couple computations of surface and subsurface processes. Both surface and subsurface water flow and solute transport modules are coded in program subroutines and functions in the Intel FORTRAN environment. The coupled model was validated by comparing its simulation results with measured data. Results showed that simulated water front advances in the furrow and water contents in the soil agreed with the observations reasonably well. Good simulations can be achieved with a relatively fine temporal resolution. Numerical oscillations can be eliminated by adopting appropriate time steps. As compared with the traditional furrow irrigation model, the proposed model can better quantify soil water and solute dynamics by considering interactions between surface and subsurface water flow and solute transport processes. The proposed model can be used as a decision tool to design and manage furrow irrigation.

1. Introduction

Furrow irrigation has been widely adopted for wide-spaced crops such as corn, cotton, and sunflower all over the world because of its low investment and low energy requirements (Chen and Feng, 2013). The application of fertilizers with irrigation water is a common practice in furrow irrigation (Ebrahimian et al., 2014). To evaluate the efficiency of fertilizer applications, a knowledge of the distribution of the fertilizer in the soil along the furrow is required. Additionally, poor quality waters, such as saline waters, have been extensively used for irrigation in arid and semi-arid areas, e.g., in the northwest of China, the Negev region of Israel, and northwest India (e.g., Oster, 1994; Chen et al., 2015; Mantell et al., 1985; Rajinder, 2004). Improper use of saline waters for irrigation may cause secondary salinization problems. To study environmental impacts of irrigation with saline waters, an accurate estimate of water flow and salt fluxes into the soil profile is also required (Crevoisier et al., 2008).

Many field experiments have been conducted to provide management recommendations for increasing the uniformity of fertilizer applications (Mailhol et al., 2001; Halvorson et al., 2002; Abbasi et al., 2003a; Adamsen et al., 2005) and controlling salinity (Evans et al., 1990; Moreno et al., 1995; Malash et al., 2008; Nagaz et al., 2013; Chen and Feng, 2013). However, field experiments are time-consuming and expensive and cannot include all relevant factors. Also, it is quite difficult to obtain general conclusions from field experiments due to the variability of soil properties, soil infiltration rates, field gradients, soil roughness, etc. (Ebrahimian et al., 2014). Mathematical models can provide an alternative approach to overcome these limitations.

In recent years, many models have been developed for quantifying water flow and solute transport both at the soil surface and in the subsurface under furrow irrigation. These models can be divided into three categories. The first group of models describes water flow in

* Corresponding author at: Center for Agricultural Water Research, China Agricultural University, Beijing, 100083, China.
E-mail address: ghuang@cau.edu.cn (G. Huang).

https://doi.org/10.1016/j.agwat.2018.11.024
Received 18 April 2018; Received in revised form 13 October 2018; Accepted 23 November 2018

furrows using either zero-inertia, kinematic-wave, or fully hydrodynamic equations and characterizes solute transport in furrows using either advection or advection-dispersion equations, while simple empirical functions are used to represent water and solute infiltration. Based on this modeling concept, many software packages such as SIRMOD (Walker, 2003) and WinSRFR (Bautista et al., 2009) have been developed for the design and management of surface irrigation. Furthermore, the software package SIFUM (Boldt et al., 1994) was developed for fertilization management under surge irrigation. However, the above-discussed models cannot describe distributions of water and solutes in soils in detail, which is important for the evaluation of the uniformity of water and fertilizer applications under furrow irrigation and the quantification of deep percolation and leaching. Also, parameters of empirical infiltration functions are event specific and cannot account, for example, for the effects of the antecedent soil moisture on infiltration (Zerihun et al., 2005). Thus, the use of empirical infiltration functions may result in an inaccurate estimation of infiltration.

The second group of models describes subsurface processes, i.e., water flow and solute transport in soils, using two-dimensional variably-saturated flow and advection-dispersion equations, respectively, while surface processes are simplified and treated as an upper boundary condition. Among these models, the HYDRUS (2D/3D) software package (mainly its two-dimensional version denoted as HYDRUS-2D (Šimůnek et al., 2008, 2016b) with appropriate boundary conditions has been widely used to evaluate water and solute dynamics in soils under furrow irrigation. Šimůnek et al. (2016b) identified some 25 papers in which HYDRUS-2D and its predecessors, such as SWMS_2D and CHAIN_2D, have been used to simulate water flow and solute transport in furrow irrigation systems. For instance, Crevoisier et al. (2008) used HYDRUS-2D to simulate water and nitrogen dynamics under alternate and conventional furrow irrigation. Siyal et al. (2012) and Šimůnek et al. (2016a) developed a new furrow boundary condition to better account for flow and transport processes in furrows. Šimůnek et al. (2016a) evaluated the effects of different fertigation strategies and furrow surface treatments on plant water and nitrogen use. Wang et al. (2014) coupled HYDRUS-2D with the EPIC crop growth module to evaluate soil water dynamics and melon growth under furrow irrigation. However, these types of models, cannot fully describe the dynamic processes of water advancement, storage, and recession during a furrow irrigation event. Additionally, interactions between surface and subsurface processes have not been fully considered in assessing model performance. These simplifications may produce inaccurate simulation results.

The third group of models, which couples two models fully describing the surface and subsurface processes and their interactions, represent an alternative way to simulate furrow irrigation systems. Some efforts to couple surface and subsurface models for furrow irrigation have been reported in the literature. For example, Wöhling and Schmitz (2007) coupled the zero-inertia model, HYDRUS-2D, and the crop model to simulate water flow and crop growth under furrow irrigation. However, they did not consider solute transport (e.g., fertilizers and salts) and their effects on crop growth. Ebrahimian et al. (2013) loosely coupled the surface model of Abbasi et al. (2003b) with HYDRUS-2D to simulate water and solute dynamics under furrow irrigation. However, their coupling procedure was not very accurate since it did not consider the mutual feedback between surface and subsurface systems. Therefore, more accurate coupling methods, i.e., the iterative coupling and full coupling methods, are required to develop more reliable furrow irrigation models (e.g., Furman, 2008).

The objectives of this study are (1) to develop a coupled model for numerically simulating water and solute dynamics under furrow irrigation by an iterative coupling of physically-based surface and subsurface models, (2) to validate the coupled model by comparing its simulation results with available experimental data, and (3) to conduct numerical tests evaluating the accuracy and efficiency of the coupled model.

2. Theory and method

2.1. Model description

2.1.1. Surface flow

Water flow in a furrow can be described using the zero-inertia equation, which is a simplified form of the full hydrodynamic equation obtained by neglecting the inertial and acceleration terms (Elliott et al., 1982). The mathematical expression of the zero-inertia equation is:

$$\frac{\partial A}{\partial t} + \frac{\partial Q}{\partial x} + \frac{\partial Z}{\partial t} = 0 \tag{1}$$

$$\frac{\partial h}{\partial x} = S_0 - S_f \tag{2}$$

where A is the cross-sectional flow area (m^2), Q is the flow rate ($m^3 s^{-1}$), Z is the infiltration volume per unit length of furrow (m^2), h is the flow depth (m), S_0 is the bottom slope of the furrow (-), S_f is the friction slope (-), x is the horizontal distance (m), and t is time (s). The friction slope is defined using the Manning equation:

$$S_f = \frac{Q^2 N^2}{c_u^2 A^2 R^{4/3}} \tag{3}$$

where N is the Manning's roughness ($m^{1/6}$), R is the hydraulic radius (m), and c_u is a dimensional constant equal to 1 when units ($m^{1/2}\ s^{-1}$) are used.

For a furrow of an arbitrary cross-section, the flow depth can be expressed as a power function of the flow area (Elliott et al., 1982):

$$h = bA^p \tag{4}$$

where b and p are furrow geometry parameters in units of ($m^{1/2p}$) and (-), respectively. Similarly, the wetted perimeter can be written as a power function of the flow area. Hence, the denominator of Eq. (3) becomes a function of A:

$$A^2 R^{4/3} = dA^f \tag{5}$$

where d and f are hydraulic section parameters in units of ($m^{5.33-2f}$) and (-), respectively. Substituting Eqs. (4) and (5) into Eq. (2), one obtains

$$\frac{\partial (bA^p)}{\partial x} = S_0 - \frac{Q^2 N^2}{dA^f} \tag{6}$$

Eqs. (1) and (6) are the basis of the surface flow model. The initial and boundary conditions are as follows:

$$\text{Initial condition: } Q(x, 0) = 0;\ A(x, t) = 0 \quad 0 \le x \le L \tag{7}$$

$$\text{Upstream boundary condition: } \begin{cases} Q(0, t) = Q_o(t) & t \le t_{co} \\ Q(x_r, t) = 0 & 0 \le x_r \le L \text{ and } t > t_{co} \\ A(x_r, t) = 0 & t_{ro} < t \le t_{rL} \end{cases} \tag{8}$$

Downstream boundary condition:

$$\begin{cases} Q(x_a, t) = 0; A(x_a, t) = 0 & 0 \le x_a \le L \text{and} t \le t_{aL} \\ Q(L, t) = 0 & t > t_{aL} \end{cases} \text{ for a blocked-end furrow,}$$

$$A(L, t) = \left[\frac{Q^2(L,t)N^2}{S_0 d}\right]^{1/f} \quad t \ge t_{aL} \quad \text{for a free-draining furrow} \tag{9}$$

where L is the furrow length (m), Q_0 is the inflow rate ($m^3\ s^{-1}$), t_{co} is the cutoff time (s), x_r is the distance of the receding tip from the upstream end (m), t_{ro} is the recession time at the upstream end (s), t_{rL} is the recession time at the downstream end (s), x_a is the advance distance (m), and t_{aL} is the advance time (s).

2.1.2. Solute transport in the furrow

Solute transport in a furrow can be described using a one-dimensional cross-sectional average dispersion equation (Cunge et al., 1980):

$$\frac{\partial AC}{\partial t} + \frac{\partial QC}{\partial x} + \frac{\partial ZC}{\partial t} = \frac{\partial}{\partial x}\left(AD_x \frac{\partial C}{\partial x}\right) \tag{10}$$

where C is the solute concentration (kg m^{-3}) and D_x is the dispersion coefficient (m^2 s^{-1}). The dispersion coefficient accounts for the dispersion due to differential advection and turbulent diffusion (Cunge et al., 1980). D_x can be written as (Abbasi et al., 2003b):

$$D_x = \alpha_x v + D_d \tag{11}$$

where α_x is the longitudinal dispersivity (m), v is the mean cross-sectional velocity (m s^{-1}), and D_d is the molecular diffusion in free water (m^2 s^{-1}). The initial and boundary conditions are as follows:

$$\text{Initial condition:}\quad C(x, 0) = 0 \quad 0 \le x \le L \tag{12}$$

$$\text{Upstream boundary condition:}\quad C(0, t) = C_o(t) \quad t \le t_{co} \tag{13}$$

$$\text{Downstream boundary condition:}\quad \frac{\partial C}{\partial x} = 0 \quad 0 \le x_a \le L \text{and} t \le t_{rL} \tag{14}$$

2.1.3. Subsurface flow

Subsurface flow in any cross-section perpendicular to the direction of surface flow can be described by using the two-dimensional Richards equation:

$$\frac{\partial \theta}{\partial t} = \frac{\partial}{\partial x_i}\left[K\left(K_{ij}^A \frac{\partial h}{\partial x_j} + K_{iz}^A\right)\right] - S \tag{15}$$

where θ is the volumetric moisture content (-), h is the pressure head (m), K is the unsaturated hydraulic conductivity (m s^{-1}), K_{ij}^A are components of a dimensionless anisotropy tensor $\boldsymbol{K}^A$, x_i and x_j are the spatial coordinates (m), and S is the sink term accounting for root water uptake.

The unsaturated hydraulic conductivity function is determined using the van Genuchten-Mualem model (Mualem, 1976; van Genuchten, 1980):

$$K(h) = K_s S_e^{0.5}[1 - (1 - S_e^{1/m})^m]^2 \tag{16}$$

$$S_e = \frac{\theta - \theta_r}{\theta_s - \theta_r} = [1 + (\alpha h)^n]^{-m} \tag{17}$$

$$m = 1 - 1/n \tag{18}$$

where K_s is the saturated hydraulic conductivity (m s^{-1}), S_e is the effective water saturation (-), θ_r and θ_s are the residual and saturated water contents, respectively (-), α is the inverse of the air-entry value (m^{-1}), and n is the pore-size distribution index (-).

The initial conditions are given in terms of pressure heads, which can be either constant or vary with the depth and distance along the furrow. The time-variable pressure head representing the flow depth in the furrow is considered as the upper boundary condition in the furrow, while an atmospheric boundary condition can be considered on the rest of the soil surface, including in the furrow when it is empty. A free drainage is considered as the bottom boundary condition in cases when the groundwater table is below the domain of interest. Otherwise, the Dirichlet boundary condition with a prescribed pressure head can be considered as the bottom boundary condition.

2.1.4. Solute transport in subsurface

Solute transport in any subsurface cross-section perpendicular to the direction of surface flow can be described by using the two-dimensional convection-dispersion equation:

$$\frac{\partial \theta c}{\partial t} = \frac{\partial}{\partial x_i}\left(\theta D_{ij} \frac{\partial c}{\partial x_j}\right) - \frac{\partial q_i c}{\partial x_i} - Sc^s \tag{19}$$

where c is the solute concentration in the soil (kg m^{-3}), q_i is the i-th component of the volumetric flux (m s^{-1}), D_{ij} is the dispersion coefficient tensor (m^2 s^{-1}), and c_s is the concentration of the sink term (kg m^{-3}).

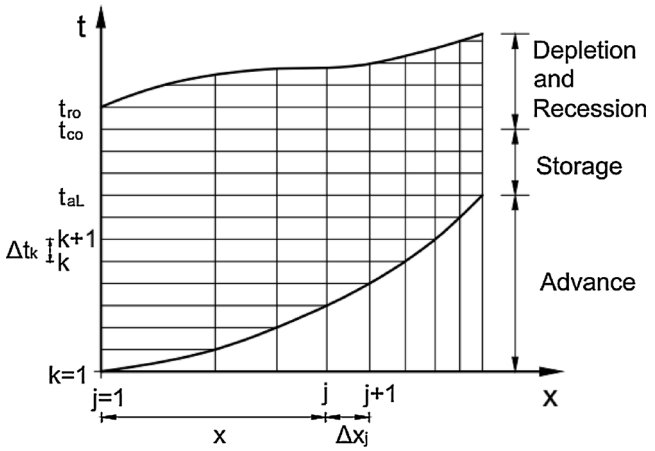

Fig. 1. Discretization of the computational domain for the numerical solution of the zero-inertia equation.

The initial conditions for concentrations can either be constant or vary with the depth and distance along the furrow. The first-type boundary condition reflecting the solute concentration in the furrow is considered as the upper boundary condition. The third-type boundary condition with the spatial derivative of the concentration equal to zero is considered as the bottom boundary condition.

2.2. Numerical solution

2.2.1. Numerical solutions for the surface and subsurface models

The zero-inertia equations, i.e., Eqs. (1) and (6), are solved using the implicit finite difference method. The discretization of the computational domain for Eqs. (1) and (6) is shown in Fig. 1. The implicit finite difference equations can be found in Appendix A. Whereas the cross-sectional average dispersion Eq. (10) is solved using the finite volume method, and the resulting linear equations can also be found in Appendix A.

The subsurface flow and transport module is based on the CHAIN_2D code (Šimůnek et al., 2008), i.e., an open source version of HYDRUS-2D. Both the two-dimensional subsurface water flow and solute transport equations subject to appropriate initial and boundary conditions were solved using the Galerkin finite element method.

2.2.2. Calculation procedures for the coupled model

The coupled model is coded in program subroutines and functions, which integrate water flow and solute transport in the furrow and CHAIN_2D (Fig. 2). The model is written in FORTRAN 90. As shown in Fig. 2, the calculation procedures are as follows:

1.First, the parameters of the surface water flow and solute transport modules are initialized and the initial input files of CHAIN_2D are read.

2.In each time step, the surface flow module is iteratively coupled with the CHAIN_2D water flow module. First, the flow water depth in each discrete node along the furrow is calculated using an estimate of the infiltration amount. The infiltration amount is assumed to be equal to that at the preceding time. Second, CHAIN_2D calculates the distribution of pressure heads in the soil profile and the cumulative infiltration amount during one time step for each node using the flow depth as the upper boundary condition. Third, the simulated cumulative infiltration amount is transferred back to the surface flow module to update the flow depth. These last two steps are repeated until the

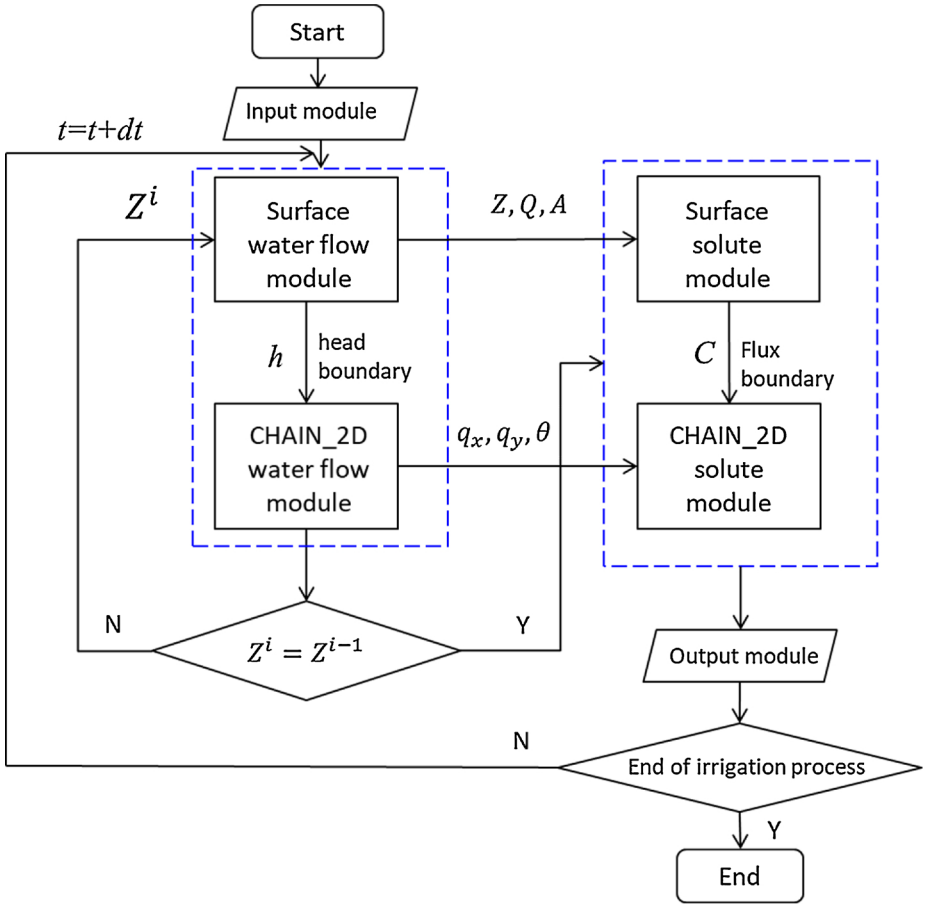

Fig. 2. Flow chart of the calculation procedure of the coupled model.

convergence criterion is fulfilled. The convergence criterion (0.001 m^2) is given as the difference in the cumulative infiltration volumes along the furrow between two adjacent iterations.

3.After the convergence criterion is satisfied, the flow modules pass selected variables (i.e., flow rates, areas, infiltrations, soil water contents, and soil water fluxes) to the solute modules to calculate solute transport processes. Unlike in water flow calculations, the interaction between the surface and subsurface solute modules is unidirectional. The surface solute module first calculates solute concentrations for each discrete node along the furrow. The CHAIN_2D solute module then calculates the distribution of solute concentrations in the soil profiles using solute concentrations in the furrow as the upper boundary conditions.

4.The results, including flow rates and areas and solute concentrations in the furrow as well as the distribution of pressure heads and concentrations in the soil profiles, are printed after the completion of solute calculations.

5.Steps (2) to (4) are repeated until the entire irrigation process is simulated.

2.3. Model validation

2.3.1. Validation of the surface flow and solute transport models

The numerical solution of the zero-inertia equation was validated against the field experimental data of Abbasi et al. (2003b) for the water advance and recession phases using the parameters given in Table 1. The numerical solution of the solute transport in the furrow was also validated by comparing simulation results with the field experimental data of Abbasi et al. (2003b). The inflow rate of 1.29 L s^{-1} and the applied solute concentration of 2.36 g L^{-1} were considered in the simulation.

Table 1
Parameters of the field experiment of Abbasi et al. (2003b).

Parameter	Value
Field length (m)	115
Field slope (m m^{-1})	0.0001
Furrow geometry parameters	
d ($m^{5.33-2f}$)	0.326
f (-)	2.789
b ($m^{1/2p}$)	0.871
p (-)	0.635
Infiltration parameters	
a (-)	0.75
k (m^3 min^{-a} m^{-1})	0.00209
c (m^3 m^{-1})	0.006
Manning roughness ($m^{1/6}$)	0.066
Cutoff time (min)	140
Solute application time (min)	140
Dispersivity (cm)	10

Note: adapted from Abbasi et al. (2003b).

The numerical solution for the solute transport model in the furrow was also evaluated using the analytical solution. For a steady uniform flow condition and given the initial condition ($C(x,0) = 0$, for $0 \le x \le L$) and boundary conditions ($C(0, t) = C_0$, $C(L, t) = 0$, for $0 \le t \le T$), the analytical solution can be expressed as (Warrick, 2003):

$$C(x, t) = \frac{C_0}{2}\left[erfc\left(\frac{x - vt}{2\sqrt{D_x t}}\right) + e^{vx/D_x} erfc\left(\frac{x + vt}{2\sqrt{D_x t}}\right)\right] \quad (20)$$

where C_0 is the inlet concentration, L is the length of the computation domain, and T is the total time (Warrick, 2003). A hypothetical

Table 2
Parameters of three irrigation laboratory experiments of Wöhling et al. (2004).

Parameters	1st irrigation	2nd irrigation	3rd irrigation
Average inflow rate (L s^{-1})	1.20	2.14	2.58
Cutoff time (h)	2.55	5.37	3.62
Furrow length (m)	26.4	26.4	26.4
Furrow slope (m m^{-1})	0.0025	0.0014	0.0015

Note: adapted from Wöhling et al. (2004).

example with the parameter values $C_0 = 1$, $L = 1$, $T = 1$, $v = 1$, and $D_x = 0.1$ was set up for this evaluation.

2.3.2. Validation of the coupled model

The coupled model was validated using the experimental data of Wöhling et al. (2004), who carried out laboratory experiments to investigate surface and subsurface flow patterns during the advance phase of furrow irrigation. A parabolic furrow, with a top width of 0.35 m and a depth of 0.184 m, was formed in an experimental tank. Fifty tensiometer probes were placed at five cross sections (x = 1.5, 6.3, 12.3, 18.3, and 24.3 m) to measure pressure heads. The soil hydraulic parameters were optimized by a MATLAB routine using the pressure head measurements at the cross section x = 12.3 m. The resulting optimized parameters of the van Genuchten-Mualem model were $\alpha = 1.4\ m^{-1}$, $n = 1.25$, $K_s = 1.95 \times 10^{-5}$ m s^{-1}, $\theta_s = 0.41$, and $\theta_r = 0.14$. More details about the experiments can be found in Wöhling et al. (2004). Three irrigation experiments were conducted with different inflow rates and bottom slopes. The detailed experimental information is shown in Table 2. The initial conditions for the subsurface flow model were determined by averaging measured pressure heads at five cross sections, which are shown in Table 3. The simulated water advance by the coupled model was compared with the measured data and with that simulated by the Wöhling's model (Wöhling et al., 2004), in which the analytical solution of the zero-inertia equation was used to describe surface water flow. Simulated pressure heads in different cross sections (i.e., x = 6.3 m and x = 18.3 m) were also compared with the measurements.

The coefficient of determination (R^2) and the root mean square error (RMSE) were used as indicators to evaluate the performance of the model validation.

2.4. Numerical tests

In the proposed coupled model, all governing equations were solved using a numerical solution. Numerical solutions can generally handle more complex initial and boundary conditions, as well as heterogeneities in soil properties, than analytical solutions. However, numerical solutions often encounter numerical problems and are stable only when they fulfill certain stability criteria, often involving limits on the spatial and temporal discretization, i.e., spatial and time steps. Generally, the accuracy of simulation results depends greatly on the time and space resolution. In our proposed model, a constant time step is used in the numerical solution of the zero-inertia equation. The space increment is determined by the difference of the calculated water front positions at two adjacent times. It should be noted that the space increment is not constant during the simulations because the velocity of the water advance decreases during the advance phase (see Fig. 1). In order to analyze the impact of the time resolution, numerical tests were conducted for time steps Δt = 30 s, 60 s, and 120 s A hypothetical case was set up for these numerical tests with its parameters given in Table 4. In this case, the sandy soil was considered and its hydraulic parameters were adopted from Vogel and Hopmans (1992). Initial soil pressure heads and solute concentrations were assumed to be uniformly distributed with values of -2.5 m and 0 g m^{-3}, respectively. The simulation results for different time steps were compared with each other. The total volume balance errors, δ, were also computed for different time steps:

$$\delta = \frac{|V_{in} - V_{total}|}{V_{in}} \times 100\% \quad (21)$$

where V_{total} is the sum of the surface water and infiltration volumes (m^3) and V_{in} is the water volume applied into the furrow (m^3).

Table 3
Average initial pressure heads at different locations used in the subsurface flow model.

Soil depth (m)	h (m) 1st irrigation	h (m) 2nd irrigation	h (m) 3rd irrigation
0.2	−4.37	−6.65	−1.74
0.3	−3.33	−5.45	−1.45
0.35	−2.83	−6.02	−1.58
0.45	−2.41	−3.94	−1.16
0.5	−2.25	−4.09	−1.19
0.6	−2.02	−4.22	−1.06
0.7	−1.97	−3.61	−0.86
0.8	−2.07	−2.72	−0.64
1.05	−3.46	−3.43	−0.68

Note: adapted from Wöhling et al. (2004).

Table 4
Parameters for the time resolution tests.

Parameter	Value
Field length (m)	100
Field slope (m m^{-1})	0.0015
Geometry parameters	
d	0.382
f	2.767
b	1.150
p	0.564
Manning roughness ($m^{1/6}$)	0.03
Inflow rate (L s^{-1})	2.0
Applied solute concentration (g L^{-1})	6.3
Cutoff time (min)	60
Solute application time (min)	60
Dispersivity (cm)	10

3. Results and discussion

3.1. Simulation results of the surface flow and solute transport models

Fig. 3 shows the comparison of the water advance and recession measured and simulated using the numerical zero-inertia model. It can

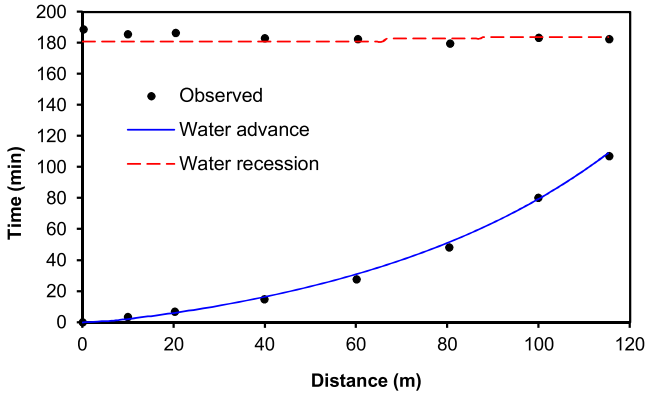

Fig. 3. Comparison of the measured (symbols) and simulated water advance (solid line) and recession (dashed line) using the zero-inertia model.

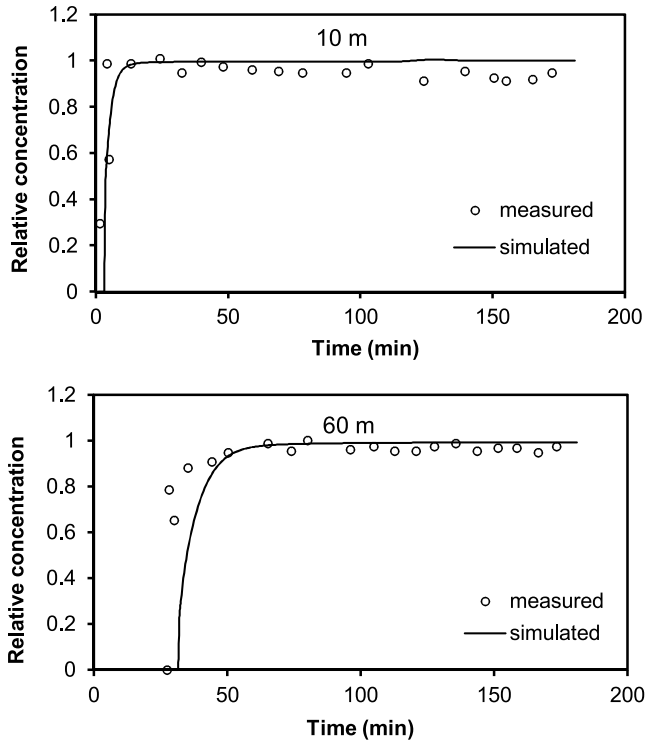

Fig. 4. Comparison of measured and simulated solute concentrations at a distance of 10 (top) and 60 (bottom) m from the furrow inlet.

be seen that the recession time was approximately the same along the furrow. This may be attributed to a small field slope and spatially relatively uniform infiltration. The simulated water advance and recession agree reasonably well with the measurements, indicating that the numerical zero-inertia model has good accuracy. The differences between the simulations and measurements may be due to the spatial and temporal variability of infiltration and roughness, and the non-uniformity of the field slope along the furrow (Abbasi et al., 2003b).

The simulated solute concentrations at the distances of 10 and 60 m from the inlet were compared with the measurements in Fig. 4. The solute concentration increased rapidly with the water advance and then reached a constant value. In general, the simulated solute concentrations were in good agreement with the measurements. Deviations between early simulated and measured values were mainly due to variations in the inflow rate, resulting in unstable solute concentrations in the irrigation water.

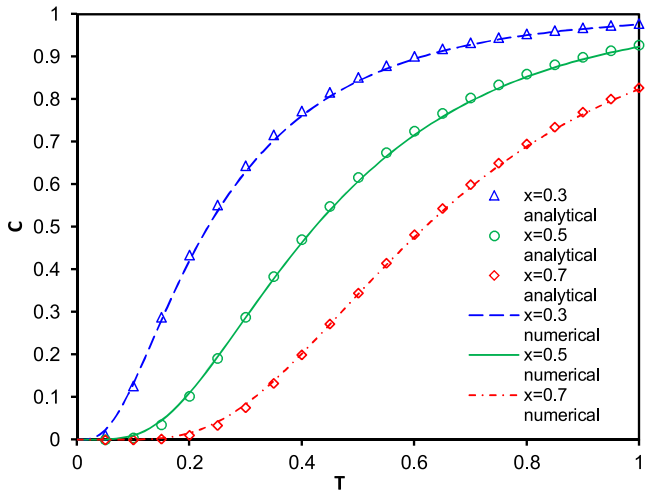

Fig. 5. Comparison of concentrations obtained using either the analytical or numerical solutions of the cross-sectional average dispersion equation.

Fig. 5 presents the comparison between analytical and numerical solutions for the cross-sectional average dispersion equation. The concentrations at different locations simulated using the numerical solution were in very good agreement with those obtained using the analytical solution. This indicates that the numerical solution has relatively high accuracy.

3.2. Performance of the coupled model

A comparison of the water advance measured and simulated using the coupled model is presented in Fig. 6. It can be seen that the

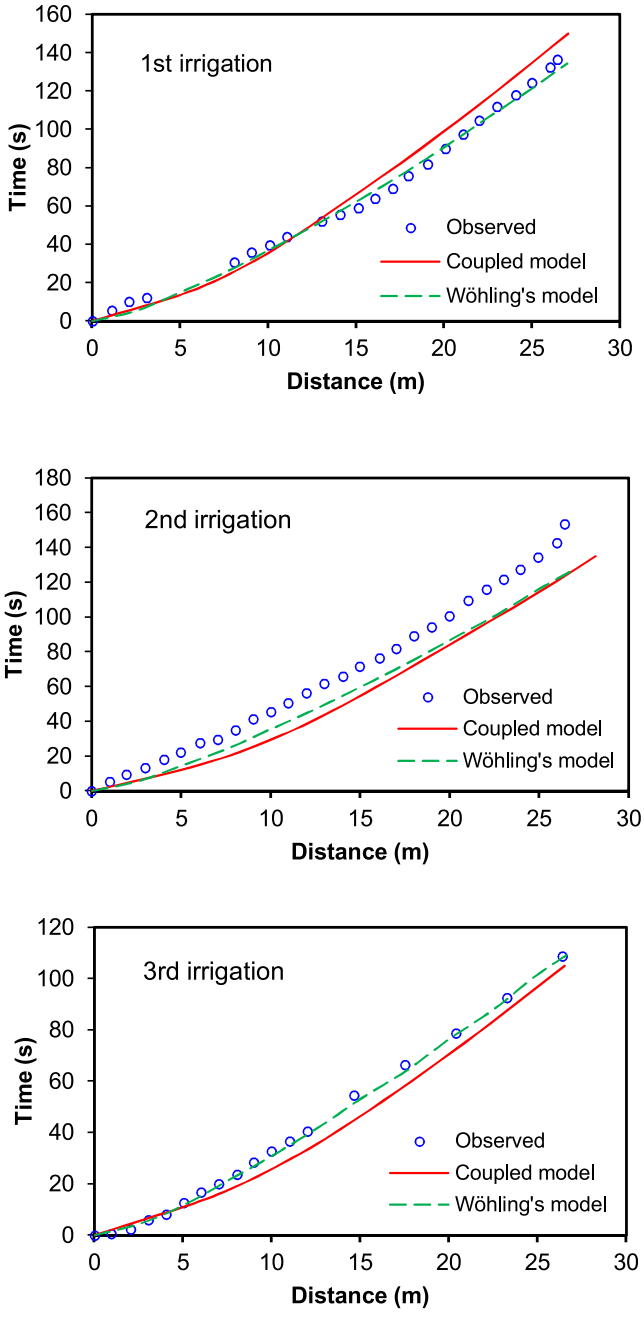

Fig. 6. Comparison of the water advance measured and simulated using the new coupled model and the Wöhling's model (Wöhling et al., 2004) for three furrow irrigation experiments.

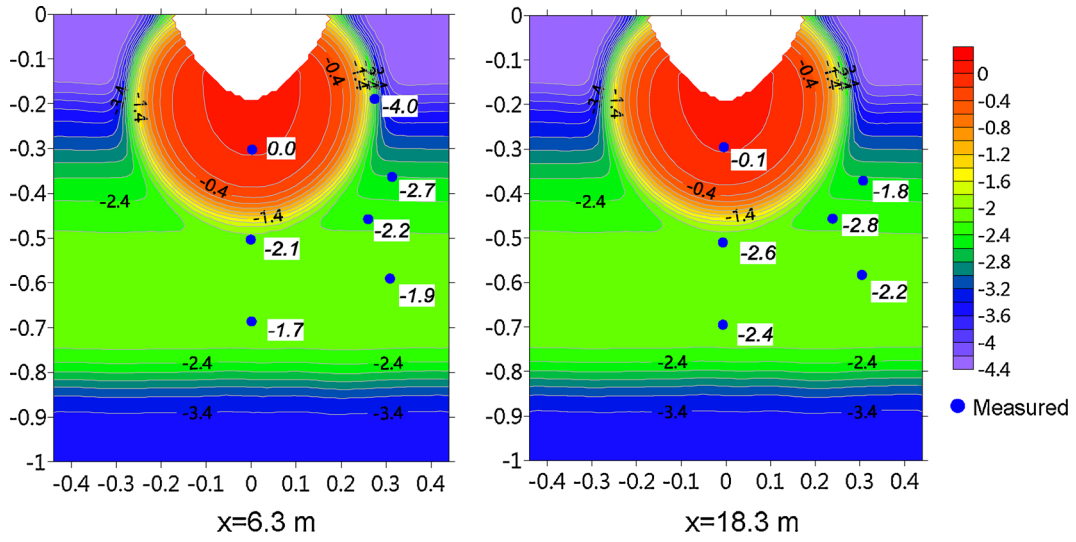

Fig. 7. Measured and simulated distributions of the pressure head in the soil profiles at distances of 6.3 (left) and 18.3 (right) m from the furrow inlet after 20 min irrigation time.

measured and simulated water advance values matched reasonably well, as reflected by the coefficient of determination R^2 of 0.99 and the RMSE of 1.02–2.73 m, implying that the coupled model has reasonable accuracy. Differences between simulations and observations may be due to the spatial variability of infiltration and roughness along the furrow. While for the first irrigation, the coupled model predicted a slightly slower water advance than measured, for the second irrigation, it predicted a faster water advance. This may be attributed to a significant increase in the initial infiltration rate caused by soil cracks that developed between the first and second irrigations (Wöhling et al., 2004).

Water advances simulated by both the coupled and Wöhling's models (Wöhling et al., 2004) are also presented in Fig. 6 for comparison. The water advance simulated by the coupled model was slightly slower than simulated by the Wöhling's model for the first irrigation and slightly faster for the second and third irrigations. This could be explained by the fact that the Wöhling's model used the analytical solution of the zero-inertia equation, whereas the numerical solution was used in the present work. The analytical solution of Wöhling assumed that the momentum could be expressed as the momentum at the center of gravity of the water body. This assumption was not needed in our numerical solution. In addition, the iterative convergence criteria used in our model was different from that of Wöhling's model. This might result in different simulation results.

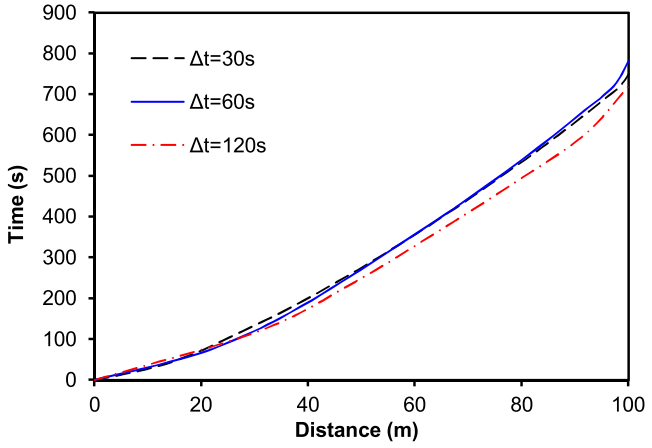

Fig. 8. Simulated water advance for time steps Δt = 30, 60, and 120 s.

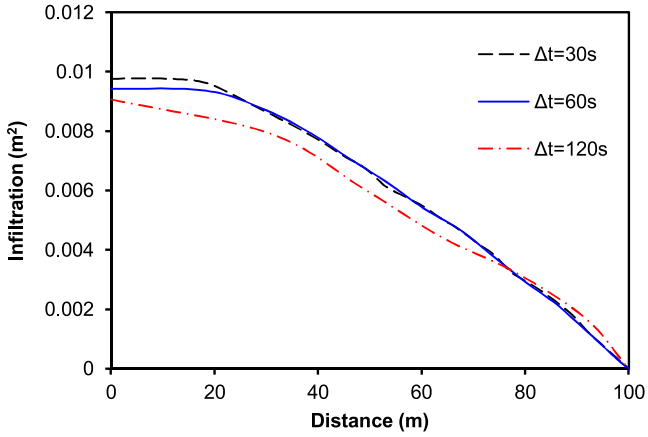

Fig. 9. Simulated cumulative infiltration along the furrow during the advance phase for time steps Δt = 30, 60, and 120 s.

Fig. 7 shows the simulated and measured pressure head distributions in soils at the cross-sections 6.3 and 18.3 m from the furrow inlet after 20 min irrigation time. In general, the simulations were in good agreement with the measurements. The discrepancy between the

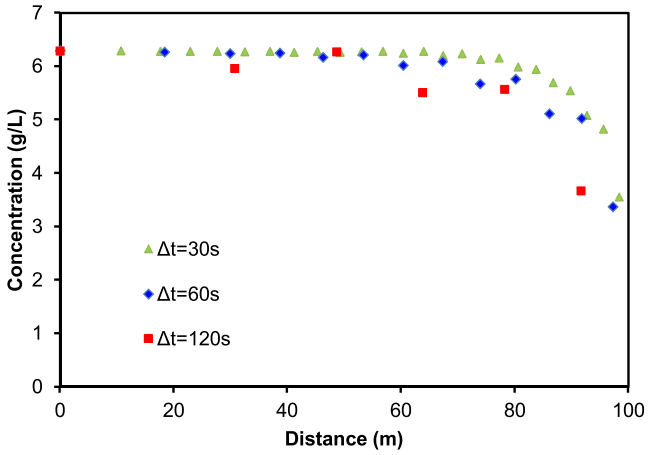

Fig. 10. Simulated solute concentrations along the furrow after 30 min for time steps Δt = 30, 60, and 120 s.

simulated and measured results may be attributed to the approximation of the initial conditions for the simulation. Similarly to Wöhling et al. (2004), the initial pressure heads over the simulation depth were obtained by interpolating measured pressure heads at nine depths (see Table 3).

3.3. Impact of the time resolution

The simulated water advances for different time step sizes Δt are presented in Fig. 8, which shows that the water advance was similar for time steps Δt = 30 and 60 s, whereas it was faster for Δt = 120 s.

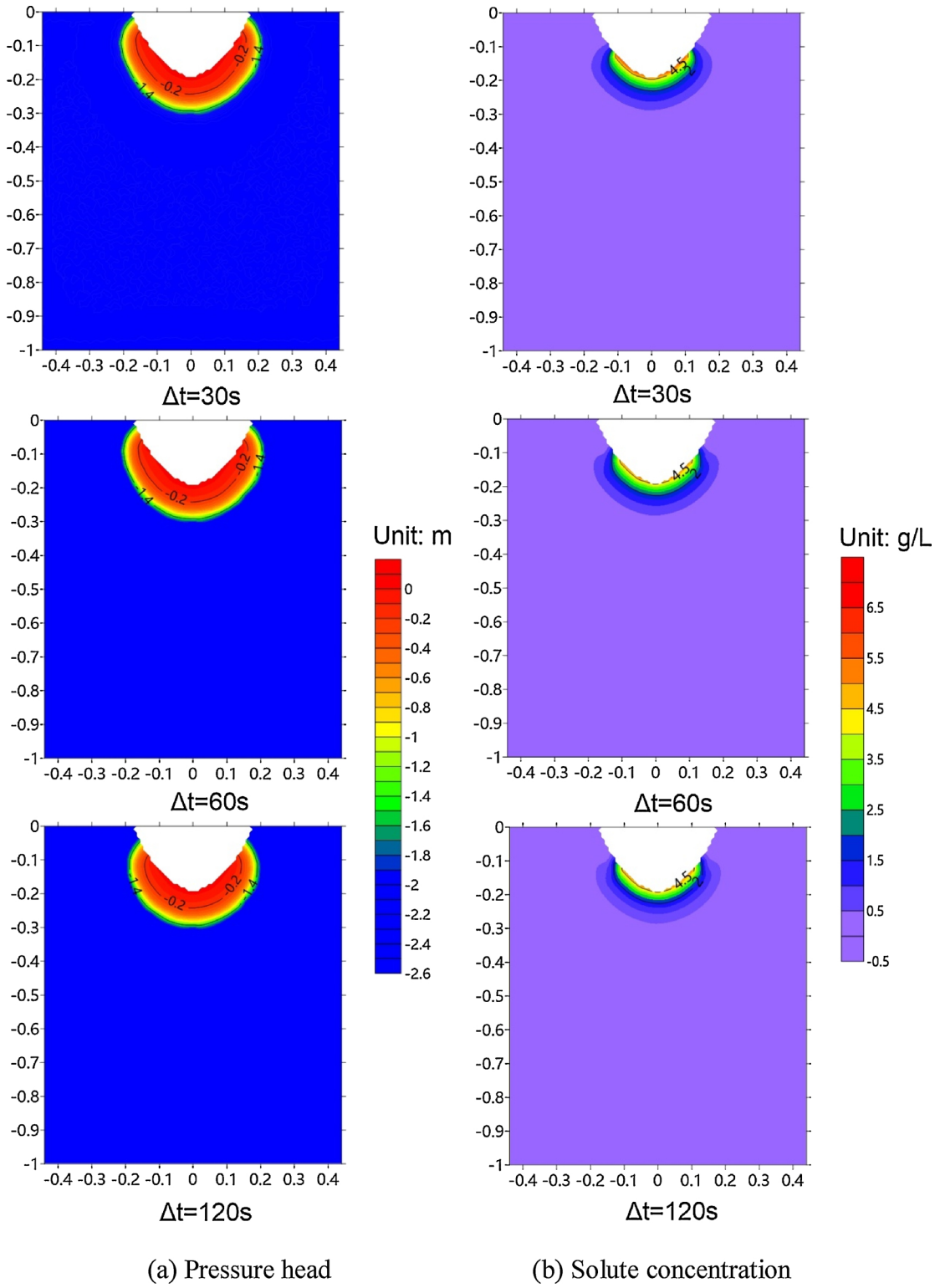

Fig. 11. Simulated pressure heads (top) and solute concentrations (bottom) in the soil profile at a distance of 50 m form the furrow inlet after 30 min irrigation time for time steps Δt = 30 (up), 60 (middle), and 120 (down) s.

Infiltration for $\Delta t = 120$ s was underestimated in comparison with those for $\Delta t = 30$ and 60 s during the water advance process (see Fig. 9), resulting in a faster water advance. The total volume balance error (Eq. 26) showed a significant increase from 0.8% for $\Delta t = 30$ s to 3.2% for $\Delta t = 120$ s. This indicates that larger time steps and space sizes (the space increment increases with the time step in the coupled model) may cause an inaccurate evaluation of infiltration and the water advance time. These results are consistent with those of Wöhling et al. (2004), who reported that the large space sizes could lead to the biased estimation of infiltration and advance time. Banti et al. (2011) also indicated that smaller space increments could result in lower volume balance errors.

Fig. 10 presents simulated solute concentrations along the furrow after 30 min irrigation time for different time steps. Significant numerical oscillations could be found in the simulation with $\Delta t = 120$ s, whereas there were no visible numerical oscillations in the simulation with $\Delta t = 30$ s. This may be attributed to the fact that larger time steps resulted in larger Peclet and Courant numbers. In our numerical tests, Peclet numbers were less than 8.0 for $\Delta t = 30$ s and less than 18.0 for $\Delta t = 120$ s. Corresponding Courant numbers were less than 1.5 for $\Delta t = 30$ s and less than 1.7 for $\Delta t = 120$ s. Similar results were also found by Abbasi et al. (2003b), who reported that no significant numerical oscillations could be found for simulations with Peclet numbers smaller than 10 and Courant numbers not larger than 1. Although the Courant number is larger than 1 in our simulations, a Courant number smaller than 2 is acceptable as the average dispersion equation (Eq. 10) is solved using an implicit scheme. It should be noted that Fig. 10 shows a decrease of solute concentrations below c_0 at the outflow end. This is the result of the numerical dispersion and not a physical phenomenon since there is no physical process in our hypothetical example that could lower concentrations below c_0.

The simulated pressure heads and solute concentrations in the soil profile after 30 min irrigation time for different time steps are shown in Fig. 11. It can be seen that simulated pressure head distributions were similar for $\Delta t = 30$ and 60 s. The wetted area for $\Delta t = 120$ s is slightly smaller than for $\Delta t = 30$ and 60 s. This further demonstrates that using the time step of 120 s may underestimate infiltration. Simulated solute concentrations for $\Delta t = 120$ s are smaller than those for $\Delta t = 30$ and 60 s. This is also attributed to the fact that the infiltration volumes for $\Delta t = 120$ s are smaller.

The required CPU time for different time steps is presented in Fig. 12, which shows that the CPU time increased significantly with the decrease of the time step. The CPU time for $\Delta t = 30$ s was 2.5 times larger than for $\Delta t = 60$ s and 9.3 times larger than for $\Delta t = 120$ s. This was mainly due to the numerical solution of the two-dimensional Richards equation and the convection-dispersion equation, i.e., for subsurface processes. Using smaller time steps resulted in having more subsurface profiles perpendicular to the direction of surface flow, requiring many more computations.

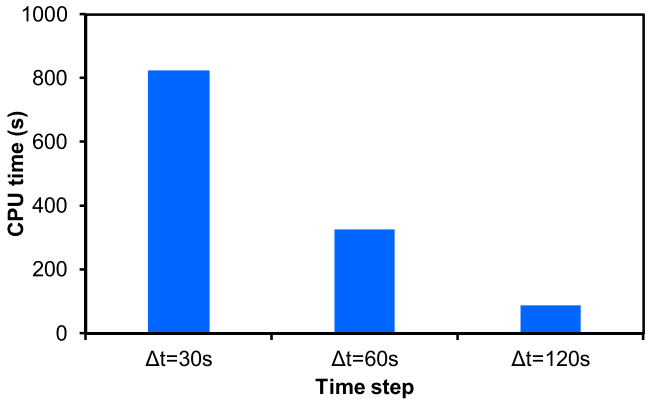

Fig. 12. CPU times for time steps $\Delta t = 30$, 60, and 120 s.

There are many ways to improve the computational efficiency. First, the numerical code can be parallelized to significantly reduce the computational time when the code is run on multiple-core processors or multiple processors. Second, if one only needs to know the cumulative infiltration amount rather than detailed water and solute distributions in soils, a simple infiltration model can be used instead of the sophisticated two-dimensional process model. For example, Bautista et al. (2016) proposed an approximate furrow infiltration model by treating the two-dimensional infiltration as a sum of a one-dimensional infiltration and edge effects. This model could obtain comparably accurate estimations of cumulative infiltration as the numerical solution of the two-dimensional Richards equation. Similarly, an empirical surface flow function can be used instead of a physically based model. Ghanbarian et al. (2018) provided theoretical insights into the exponent in the empirical power-law advance-time curve, which is widely used in surface irrigation. However, improving the computational efficiency may not be a big concern in the current situation when significant computational resources are often readily available.

It should be pointed out that the proposed model is highly computationally efficient. This is because the subsurface water flow and solute transport modules in the coupled program are called directly from the overland flow module, rather than passing various variables through external HYDRUS files (as done in Wöhling et al., 2004; Zerihun et al., 2005; Wöhling and Schmitz, 2007). In addition, the modular programming method makes it easy to optimize each part of the model separately. The proposed model can simulate the water and solute dynamics of all phases of a furrow irrigation event by considering interactions between surface and subsurface water flow and solute transport processes. It can also provide a more detailed distribution of both water and solute in soils in comparison with traditional furrow irrigation models. Hence the proposed model is a useful tool for water and fertilizer management under furrow irrigation.

In this study, crop growth processes were not considered in the coupled model. However, the effect of irrigation and fertigation on crop growth using different irrigation techniques is always an important factor for water management at different scales. Therefore, future research should focus on incorporating the crop growth module into the coupled model to allow simultaneous simulations of soil water and solute dynamics, as well as crop growth during the entire growing season.

4. Summary and conclusions

A coupled model for simulating water flow and solute transport under furrow irrigation was developed. In the model, surface water flow and solute transport were described using the zero-inertia equation and the cross-sectional average dispersion equation, respectively. The two-dimensional Richards and advection-dispersion equations, respectively, were used to simulate water flow and solute transport in soils. The surface and subsurface models were coupled using an iterative coupling method and were coded in program subroutines and functions in the Intel FORTRAN environment. The proposed model was validated by comparing its simulation results with measured data from laboratory and field experiments, as well as with other available models. Numerical tests were conducted to analyze the accuracy and efficiency of the coupled model. When smaller time steps were used, more robust simulations without significant numerical oscillations and dispersion were obtained, albeit at a higher computational cost. The proposed model can simulate all phases of an irrigation event and provide detailed quantification of both water and solute dynamics under furrow irrigation by considering interactions between surface and subsurface water flow and solute transport processes. The proposed model can serve as a decision tool for the design and management of furrow irrigation.

Acknowledgments

This research was jointly supported by the National Key R&D Program of China (No. 2017YFC0403301) and National Natural Science Foundation of China (Nos. 51639009, 51621061, 51125036).

Appendix A

The implicit finite difference schemes for Eqs. (1) and (6) can be expressed as (Elliott et al., 1982):

$$H_j \Delta A_j^{k+1} + B_j \Delta A_{j+1}^{k+1} + C_j \Delta Q_j^{k+1} + D_j \Delta Q_{j+1}^{k+1} = G_j \tag{A1}$$

$$H_j' \Delta A_j^{k+1} + B_j' \Delta A_{j+1}^{k+1} + C_j' \Delta Q_j^{k+1} + D_j' \Delta Q_{j+1}^{k+1} = G_j' \tag{A2}$$

where

$$H_j = \phi \frac{\Delta x_j}{\Delta t} + \psi \frac{\Delta x_{j-1}}{\Delta t},\quad B_j = (1-\phi-\psi)\frac{\Delta x_j}{\Delta t},\quad C_j = -\psi,\quad D_j = \psi,$$

$$G_j = \left[\phi \frac{\Delta x_j}{\Delta t} + (1-\phi)\frac{\Delta x_{j-1}}{\Delta t}\right](A_{j+1}^k + Z_{j+1}^k - A_j^k - Z_j^k) + Q_j^k - Q_{j+1}^k,$$

$$H_j' = -bp(A_j^k)^{p-1} - \phi f \frac{S_f^j}{A_j^k}\Delta x_j,\quad B_j' = bp(A_{j+1}^k)^{p-1} - (1-\phi) f \frac{S_f^{j+1}}{A_{j+1}^k}\Delta x_j,$$

$$C_j' = 2\phi \frac{S_f^j}{Q_j^k}\Delta x_j,\quad D_j' = 2(1-\phi)\frac{S_f^{j+1}}{Q_{j+1}^k}\Delta x_j,$$

$$G_j' = b[(A_j^k)^p - (A_{j+1}^k)^p] + \Delta x_j [S_0 - \phi S_f^j - (1-\phi) S_f^{j+1}],$$

$$\Delta A = A^{k+1} - A^k,\quad \Delta Q = Q^{k+1} - Q^k,\quad \text{and}\quad S_f^j = \frac{(Q_j^k)^2 N^2}{d(A_j^k)^f}, \tag{A3}$$

in which j is the node index, k is the timeline index, and φ and ψ are the space and time weighting factors, respectively. In this study, φ and ψ were considered with values of 0.5 and 0.6, respectively.

When the furrow is discretized into N cells, there are $2N$ linear algebraic equations and $2N$ unknowns. The linear Eqs. (A1) and (A2), combined with the initial and boundary conditions, are solved using the Gaussian elimination method.

Using the finite volume method, the cross-sectional average dispersion Eq. (10) can be decretized as:

$$a_W C_{j-1}^{k+1} + a_P C_j^{k+1} + a_E C_{j+1}^{k+1} = b_P \tag{A4}$$

where

$$a_W = -\frac{\frac{Q_{j-1}^k + Q_j^k}{2}\frac{\Delta t}{2}}{} - \frac{\frac{D_{j-1}^k + D_j^k}{2}\cdot\frac{A_{j-1}^k + A_j^k}{2}\frac{\Delta t}{\Delta x_{j-1}}}{},$$

$$a_E = \frac{\frac{Q_{j+1}^k + Q_j^k}{2}\frac{\Delta t}{2}}{} - \frac{\frac{D_{j+1}^k + D_j^k}{2}\cdot\frac{A_{j+1}^k + A_j^k}{2}\frac{\Delta t}{\Delta x_j}}{},$$

$$a_P = A_j^k\left(\frac{\Delta x_{j-1} + \Delta x_j}{2}\right) + Z_j^k\left(\frac{\Delta x_{j-1} + \Delta x_j}{2}\right) + \left(\frac{Q_{j+1}^k + Q_{j-1}^k}{2}\right)\frac{\Delta t}{2},$$

$$\Delta t\left(\frac{D_{j+1}^k + D_j^k}{2}\cdot\frac{A_{j+1}^k + A_j^k}{2}\frac{1}{\Delta x_j} + \frac{D_{j-1}^k + D_j^k}{2}\cdot\frac{A_{j-1}^k + A_j^k}{2}\frac{1}{\Delta x_{j-1}}\right)$$

$$\text{and}\quad b_P = (A_j^k C_j^k + Z_j^k C_j^k)\left(\frac{\Delta x_{j-1} + \Delta x_j}{2}\right), \tag{A5}$$

in which j is the node index and k is the timeline index. Variables A, Z, and Q are obtained from the numerical solution of the zero-inertia equation. For N cells, there are N linear algebraic equations and N unknowns. Similarly as for water flow, the linear Eq. (A4), combined with the initial and boundary conditions, are solved using the Gaussian elimination method.

References

Abbasi, F., Adamsen, F.J., Hunsaker, D.J., Feyen, J., Shouse, P., van Genuchten, M.T., 2003a. Effects of flow depth on water flow and solute transport in furrow irrigation: field data analysis. J. Irrig. Drain. Eng. 129 (4), 237–245.

Abbasi, F., Šimůnek, J., van Genuchten, M.Th., Feyen, J., Adamsen, F.J., Hunsaker, D.J., Strelkoff, T.S., Shouse, P., 2003b. Overland water flow and solute transport: model development and field-data analysis. J. Irrig. Drain. Eng. 129 (2), 71–81.

Adamsen, F.J., Hunsaker, D.J., Perea, H., 2005. Border strip fertigation: effect of injection strategies on the distribution of bromide. Trans. ASAE 48 (2), 529–540.

Banti, M., Zissis, T., Anastasiadou-Partheniou, E., 2011. Furrow irrigation advance simulation using a surface-subsurface interaction model. J. Irrig. Drain. Eng. 137 (5), 304–314.

Bautista, E., Clemmens, A.J., Strelkoff, T.S., Schlegel, J.L., 2009. Modern analysis of surface irrigation systems with WINSRFR. Agric. Water Manage. 96, 1146–1154.

Bautista, E., Warrick, A.W., Schlegel, J.L., Thorp, K.R., Hunsaker, D.J., 2016. Approximate furrow infiltration model for time-variable ponding depth. J. Irrig. Drain. Eng. 142 (11), 04016045.

Boldt, A.L., Watts, D.G., Eisenhauer, D.E., Schepers, J.S., 1994. Simulation of water applied nitrogen distribution under surge irrigation. Trans. ASAE 37 (4), 1157–1165.

Chen, L.J., Feng, Q., 2013. Soil water and salt distribution under furrow irrigation of saline water with plastic mulch on ridge. J. Arid Land 5 (1), 60–70.

Chen, L.J., Feng, Q., Li, F.R., Li, Ch.Sh, 2015. Simulation of soil water and salt transfer under mulched furrow irrigation with saline water. Geoderma. 241–242 87–96.

Crevoisier, D., Popova, Z., Mailhol, J.C., Ruelle, P., 2008. Assessment and simulation of water and nitrogen transfer under furrow irrigation. Agric. Water Manage. 95, 354–366.

Cunge, J.A., Holly, F.M., Verwey, A., 1980. Practical Aspects of Computational River Hydraulics. Pitman, London.

Elliott, R.L., Walker, W.R., Skogerboe, G.V., 1982. Zero-inertia modeling of furrow irrigation advance. J. Irrig. Drain. Div. 108 (3), 179–195.

Ebrahimian, H., Liaghat, A., Parsinejad, M., Playán, E., Abbasi, F., Navabian, M., 2013. Simulation of 1D surface and 2D subsurface water flow and nitrate transport in alternate and conventional furrow fertigation. Irrig. Sci. 31 (3), 301–316.

Ebrahimian, H., Keshavarz, M.R., Playán, E., 2014. Surface fertigation: a review, gaps and needs. Span. J. Agric. Res. 12 (3), 820–837.

Evans, R.G., Smith, G.J., Oster, J.D., Myers, B.A., 1990. Saline water application effects on furrow infiltration of red-brown earths. Trans. ASAE 33 (5), 1563–1572.

Furman, A., 2008. Modeling coupled surface–subsurface flow processes: a review. Vadose

Zone J. 7 (2), 741–756.
Ghanbarian, B., Ebrahimian, H., Hunt, A.G., van Genuchten, M.Th, 2018. Theoretical bounds for the exponent in the empirical power-law advancetime curve for surface flow. Agric. Water Manage. 210, 208–216.
Halvorson, A.D., Follett, R.F., Bartolo, M.E., Schweissing, F.C., 2002. Nitrogen fertilizer use efficiency of furrow-irrigated onion and corn. Agron. J. 94, 442–449.
Mantell, A., Frenkel, H., Meiri, A., 1985. Drip irrigation of cotton with saline-sodic water. Irrig. Sci. 6, 95–106.
Mailhol, J.C., Ruelle, P., Nemeth, I., 2001. Impact of fertilization practices on nitrogen leaching under irrigation. Irrig. Sci. 20 (3), 139–147.
Malash, N.M., Flowers, T.J., Ragab, R., 2008. Effect of irrigation methods, management and salinity of irrigation water on tomato yield, soil moisture and salinity distribution. Irrig. Sci. 26, 313–323.
Moreno, F., Cabrera, F., Andrew, L., Vaz, R., Martin-Aranda, J., Vachaud, G., 1995. Water-movement and salt leaching in drained and irrigated marsh soils of Southwest Spain. Agric. Water Manage. 27 (1), 25–44.
Mualem, Y., 1976. A new model for predicting the hydraulic conductivity of unsaturated porous media. Water Resour. Res. 46 (12), 513–522.
Nagaz, K., Toumi, I., Masmoudi, M.M., Mechlia, N.B., 2013. Comparative effects of drip and furrow irrigation with saline water on the yield and water use efficiency of potato (solanum tuberosum l.) in arid conditions of Tunisia. Agric. J. 6 (4), 501–510.
Oster, J.D., 1994. Irrigation with poor quality water. Agric. Water Manage. 25 (3), 271–297.
Rajinder, S., 2004. Simulations on direct and cyclic use of saline waters for sustaining cotton–wheat in a semi-arid area of north-west India. Agric. Water Manage. 66, 153–162.
Šimůnek, J., van Genuchten, M.Th., Šejna, M., 2008. Development and applications of the HYDRUS and STANMOD software packages, and related codes. Vadose Zone J. 7 (2), 587–600.
Šimůnek, J., Bristow, K.L., Helalia, S.A., Siyal, A.A., 2016a. The effect of different fertigation strategies and furrow surface treatments on plant water and nitrogen use. Irrig. Sci. 34 (1), 53–69.
Šimůnek, J., van Genuchten, M.Th., Šejna, M., 2016b. Recent developments and applications of the HYDRUS computer software packages. Vadose Zone J. 15 (7).
Siyal, A.A., Bristow, K.L., Šimůnek, J., 2012. Minimizing nitrogen leaching from furrow irrigation through novel fertilizer placement and soil management strategies. Agric. Water Manage. 115, 242–251.
van Genuchten, M.Th., 1980. A closed-form equation for predicting the hydraulic conductivity of unsaturated soils. Soil Sci. Soc. Am. J. 44, 892–898.
Vogel, T., Hopmans, J.W., 1992. Two-dimensional analysis of furrow infiltration. J. Irrig. Drain Eng. 118 (5), 791–806.
Walker, W.R., 2003. SIRMOD III—surface irrigation simulation, evaluation and design: user's guide and technical documentation. Dept. of Biological and Irrigation Engineering, Utah State Univ., Logan, Utah.
Wang, J., Huang, G., Zhan, H., Mohanty, B.P., Zheng, J., Huang, Q., Xu, X., 2014. Evaluation of soil water dynamics and crop yield under furrow irrigation with a two-dimensional flow and crop growth coupled model. Agric. Water Manage. 141, 10–22.
Warrick, A.W., 2003. Soil water dynamics. Oxford Univ Press, NY.
Wöhling, Th., Singh, R., Schmitz, G.H., 2004. Physically based modeling of interacting surface-subsurface flow during furrow irrigation advance. J. Irrig. Drain. Eng. 130 (5), 349–356.
Wöhling, Th., Schmitz, G.H., 2007. Physically based coupled model for simulating 1D surface-2D subsurface flow and plant water uptake in irrigation furrows.I: model development. J. Irrig. Drain. Eng 130 (5), 349–356.
Zerihun, D., Furman, A., Warrick, A.W., Sanchez, C.A., 2005. Coupled surface-subsurface flow model for improved basin irrigation management. J. Irrig. Drain. Eng. 131 (2), 111–128.